IEEE Access
Multidisciplinary | Rapid Review | Open Access Journal

Received 10 July 2024, accepted 26 July 2024, date of publication 30 July 2024, date of current version 7 August 2024.

Digital Object Identifier 10.1109/ACCESS.2024.3435711

RESEARCH ARTICLE

Identification of Critical Issues in Angle, Voltage, and Frequency Stability of the Nepal Power System

RASHNA SHRESTHA[1], AMRIT PARAJULI[1], MANISHA BASUKALA[2], AND SAMUNDRA GURUNG[1], (Member, IEEE)
[1]Department of Electrical and Electronics Engineering, Kathmandu University, Dhulikhel 6250, Nepal
[2]Department of Mechanical Engineering, Kathmandu University, Dhulikhel 6250, Nepal

Corresponding author: Samundra Gurung (samundra.gurung@ku.edu.np)

This work was supported by the Young Scientist Grant by Nepal Academy of Science and Technology.

ABSTRACT After end of decades of loadshedding, the power system of Nepal is moving towards the scenario of self-sufficiency. The Government of Nepal has formulated a policy to add 20 GW of hydropower in the next ten years, making a ten-fold increase compared to the current capacity. Therefore, there is a high need for the assessment of the power system stability of the current Nepal grid to mitigate any potential issues that can occur due to the addition of this huge generation. This paper conducts a comprehensive assessment of the power system stability namely voltage (static), angle (transient and small signal), and frequency stability. The proposed assessment methodology consists of three stages: the first stage constitutes the selection and modeling of the components (generator, load, line, excitation system, governor, renewable energy resources) of the power system of Nepal. The second stage then uses the stability assessment tools: time domain simulations for frequency and transient stability, modal (eigenvalue) analysis for small signal stability and voltage stability, and sensitivity analysis for identification of critical areas prone to instability. The result shows that the current grid of Nepal has a low margin of the small signal stability. The critical clearing time of the system is approximately 0.51s. The result also show that there are five potential voltage instability areas in Nepal but is robust in terms of the frequency stability. Additionally, the integration of photovoltaic generation to the Nepal grid has also been studied in this paper. The study shows that the margin of the low frequency oscillatory stability decreases with the penetration of photovoltaic generation of the power grid of Nepal.

INDEX TERMS Nepal grid, photovoltaic generation, power system stability, sensitivity analysis.

NOMENCLATURE

ABBREVIATIONS

GoN	Government of Nepal.
RES	Renewable energy resources.
SSS	Small signal stability.
PVG	Photovoltaic generation.
NEA	Nepal electrical authority.
UFLS	Under frequency load shedding.
PSS	Power system stabilizer.

SYMBOLS

f_{nadir}	Frequency nadir [Hz.].
f_{COI}	Center of inertia frequency [Hz.].
f_{max}	Maximum system frequency [Hz.].
$RoCoF$	Rate of Change of Frequency [Hz/s].
$RoCoF+$	Positive change in rate of Change of Frequency [Hz/s].
$RoCoF-$	Negative change in rate of Change of Frequency [Hz/s].
λ	Eigenvalue related to the modal voltage stability.
Λ_i	Eigenvalue of i^{th} mode related to small signal stability.

The associate editor coordinating the review of this manuscript and approving it for publication was Nagesh Prabhu.

α_i	Damping constant of the i^{th} mode.
ω_i	Frequency of oscillation of the i^{th} [rad./s].
ξ_i	Damping ratio of the i^{th} mode.
f_r	Nominal frequency [Hz.].
ΔP_d	Active power disturbance [pu.].
H	Inertia constant [s].
TSI	Transient Stability Index.
P_{ki}	Participation factor of k^{th} bus in the i^{th} mode.
P_{li}	Participation factor of the l^{th} line in the i^{th} mode.
T_{cl}	Critical clearing time [s].
OS	Overshoot in percentage.
US	Undershoot in percentage.
T_s	Settling time [s].
ΔV	Incremental change in the bus voltage [pu.].
ΔQ	Incremental change in the bus reactive power [MVAR].

I. INTRODUCTION

A. MOTIVATION

The power system worldwide is rapidly changing due to the integration of huge renewable energy resources (RESs), addition of new technologies such as electric vehicles, electric storage etc which have all sparked concerns the about the grid stability. Power system stability is defined as the ability of the system to maintain a permissible state of equilibrium following a disturbance [1]. The grid stability is absolutely vital without which an electrical network cannot operate.

Nepal is a rich country in hydropower resources and the Government of Nepal (GoN) aims to improve the country economy by proliferating hydropower projects, increasing the domestic electrical consumption, and significantly enhancing the power export to neighbouring countries, particularly India, Bangladesh and Bhutan [2]. As a result, the power system of Nepal is seeing a surge in generation and load after end of years of loadshedding. Recently, the country has installed long and extra high voltage lines upto 400kV and has also begun to export the power to India during the wet season. Moreover, the GoN has set an ambitious goal to integrate 20 GW of hydropower capacity (around 10 times the current capacity) into the grid within the next decade [2]. However, this rapid increase in generation and load can cause stability challenges, including constraints on the transmission power transfer capability, potential loadshedding due to reaching of under-frequency stability and voltage stability limits, and blackouts in extreme cases. Despite these critical concerns, there has been limited research focus on investigating the stability of the Nepal power grid.

B. LITERATURE REVIEW

Power system stability can be traditionally categorized into three main groups: Angle, Voltage, and Frequency stability [3]. Angle stability can be further divided into transient and small-signal stability (SSS). Transient stability is the ability of the power system to remain in synchronism after a disturbance and SSS is the ability of a power system to maintain oscillatory stability under small disturbances (load change, excitation system change etc). Voltage stability refers to the ability of the power system to remain within the acceptable voltage limits after a disturbance. This can have short-term and long-term dynamics [4]. The ability of the power system to keep the frequency within acceptable limits following an outage is called frequency stability. There have been numerous studies done on stability analysis of different countries. The authors of [5] have studied the impact of photovoltaic generation (PVG) in the Western U.S. interconnection; their research shows that the PVG can have both positive and detrimental impacts on the steady state and transient stability of the considered system depending on the locations. The same research team [6] analyzed the impact of PVG in the Western U.S. interconnection with respect to SSS and their result shows that the PVG reduces the system damping. A meta-heuristic based optimization method is used to optimize the parameters of power system oscillation damping controller and power system stabilizers (PSSs) installed at generating stations to improve the damping ratio of the Western U.S Interconnection system in [7]. The author's proposed method was able to significantly improve the system SSS margin. A support vector machine method to obtain the real-time transient stability assessment of a section of power grid of China is studied in [8]. The investigation of the voltage stability margin of a metropolitan area in South Korea is studied in [9]. A probabilistic-based transient stability assessment of the Korean power system is described in [10]. The authors state that the proposed method provides statistical information and thus is highly useful to the system planners. The voltage stability assessment of the Kenyan power system is done in [11] where the authors have identified the voltage instability-prone areas. The authors of [12] have studied the impact of concentrated PVG and distributed PVG in the voltage stability of a weak grid (Kenya power system). Their result shows that the dispersed PVG provided a better voltage stability margin than the centralized PVG. The authors of [13] have proposed a voltage stability assessment using ensemble sparse oblique regression tree method for operation optimization considering voltage stability constraints. Their result shows that the proposed method can improve the voltage stability margin for both IEEE test system and a real world power system. The researchers of [14] have analyzed the frequency stability assessment of the combined Ireland and Northern Ireland power systems under the proliferation of renewable generation. The paper concluded that the protection settings need to be changed and inertia-emulating controllers should be installed in the system. The frequency stability assessment of the Israeli power system was performed in [15]. The result shows that the Israel power grid can maintain the system frequency within the prescribed limit even after a large generator outage. The researchers of [16] have investigated the impact of the wind system in the Croatia power grid. The authors' study shows that the mesh connection of the grid can decrease the

initial rate of change of frequency. A study of the stability of the Baltic power system is done in [17]. The author's study shows that the system frequency limit is violated under a large disturbance but the angle stability is within the limits of the studied system. The authors of [18] have proposed a method to find the optimal size and location of Battery Energy Storage Systems under uncertainty. The results of their analysis show that the proposed method was able to keep the system's minimum frequency within the limits after a major outage.The impact of investment in Battery energy storage systems in Australia's low-carbon National Electricity Market has been studied in [19]. The result show that the system inertia increases by five-fold due to this investment.

The power grid of Nepal is responsible to ensure a reliable power source for all consumers in the country. It is also linked to India's transmission systems and allows the import and export of electricity between the two countries. The Nepal Electricity Authority (NEA) is the singular entity responsible for planning and managing the power grid of Nepal. At present, the power system of Nepal has a total installed generation capacity of approximately 2.68 GW, with a peak load demand of around 2.171 GW [2]. As stated above, huge generation has been added to the power system of Nepal; however, very limited work has focused on the assessment of the Nepal power grid stability aspects, including voltage stability [20], [21], SSS [22], transient [23] and frequency stability [24]. Moreover, existing studies often pertain to smaller bus sizes [20], [21], lack clear identification of critical SSS modes [22] or employ reduced-order models [23], [24].

C. CONTRIBUTION AND PAPER ORGANIZATION

Hence, given the increasing complexity of the power grid of Nepal, a comprehensive assessment of its stability under various scenarios is imperative. This paper aims to fulfill the research gaps outlined above and therefore, the contributions of this study are as follows:

- Detailed modeling and simulation of power system dynamics of the power grid of Nepal.
- A first of its kind of study to conduct a comprehensive stability assessment of the Nepal power grid encompassing Voltage Stability (Static), Angle Stability (Transient and SSS), and Frequency Stability under the current state, varying load conditions, and N-1 contingency scenarios.
- This study also analyzes the impact of renewable energy resources in the electrical stability of the Nepal grid.
- Proposal of indices based on sensitivity analysis for the identification of power system parameters which can have detrimental impact on the power system stability.
- Recommendations for improving the stability margin of the current power grid of Nepal.

The organization of this paper are as follows: Section II introduces the stability indices followed by Section III which describes the system modeling of the Nepal power system and the proposed methodology for the assessment of stability. Section IV provides the analyzed results followed by the conclusions of this study in Section V.

II. THEORETICAL BACKGROUND

A. FREQUENCY STABILITY

The system frequency after a disturbance (typically generator and load outage) can be quantified using two frequency stability indices: Frequency nadir (f_{nadir}) and Rate of Change of Frequency ($RoCoF$). It is desirable to have a high f_{nadir} as a lower value may lead to Under Frequency Load Shedding (UFLS) and blackouts [25]. Similarly, a high value of $RoCoF$ denotes a faster frequency decline and may lead to the tripping of power system protection relays which results in conditions of loadshedding and islanding. The system frequency under disturbance will be different at all locations, therefore a center of inertia frequency (f_{COI}) is commonly used to study frequency stability which provides an average representation and is given by [26]:

$$f_{COI} = \frac{\sum_{i=1}^{N} H_i S_i f_i}{\sum_{i=1}^{N} H_i S_i} \tag{1}$$

where H_i, S_i, f_i, and N are the inertia constant of the i^{th} generator, apparent MVA of the i^{th} generator, frequency at the i^{th} location, and number of generators in the system respectively.

The system $RoCoF$ can be computed using [27]:

$$RoCoF = \frac{\Delta P_d f_r}{2H} \tag{2}$$

where ΔP_d and f_r are the active power disturbance in p.u and nominal system frequency in Hz respectively.

B. ANGLE STABILITY

1) SMALL SIGNAL STABILITY

Small signal stability is the behavior of the power system under small disturbances and is primely related to oscillatory stability in the modern power system [1]. It is widely studied using the modal/eigenvalue analysis.

Let $\Lambda_i = \alpha_i \pm j\omega_i$ be the i^{th} eigenvalue obtained from modal analysis with α_i as damping constant and ω_i as the frequency of oscillation; The damping factor ξ_i can then be computed using [3]:

$$\xi_i = \frac{-\alpha_i}{\sqrt{\alpha_i^2 + \omega_i^2}} \tag{3}$$

The modes are said to be critical if the values of ξ_i are less than 5% in the present study [28]. The lower value of ξ_i results in larger oscillations and longer settling time, and a negative value suggests an undamped (unstable) response.

2) TRANSIENT STABILITY

The transient stability is linked to the system response after a large disturbance and can be quantified using the critical

clearing time (T_{cl}) and the Transient stability index (TSI). The TSI for a particular generator is given by [29]:

$$TSI = \frac{360 - \delta_{max}}{360 + \delta_{max}} \tag{4}$$

where δ_{max} is the maximum angular difference of a generator with respect to the reference machine.

A higher value of TSI suggests a better transient stability margin whereas a negative value signifies that the system is transient-unstable. Similarly, a higher value of T_{cl} suggests a better transient stability margin of the power system.

C. VOLTAGE STABILITY

Voltage stability is chiefly connected to the availability of the system to adequately supply reactive power to improve the voltage profile following a disturbance. There are numerous methods to assess the system voltage strength but this paper utilizes modal analysis for voltage stability [3] as it provides a system-level analysis unlike conventional methods such as PV and QV curves which are limited to the bus level [30].

The power flow equations can be linearized and rewritten in the form as [3]:

$$\Delta V = J_R^{-1} \Delta Q \tag{5}$$

where ΔV is the incremental change in bus voltage due to the incremental change in the bus reactive power ΔQ, and J_R is the reduced Jacobian matrix.

The relationship between the vector of modal voltage variations (v_i) and the reactive power variation (q_i) can be computed using [3]:

$$v_i = \frac{q_i}{\lambda_i} \tag{6}$$

where λ_i is the i^{th} eigenvalue. It can be seen from Equation (6) that when $\lambda > 0$, the system voltage and reactive power change are in the same direction which means that the system is stable. Moreover, the smaller the value of λ, the larger the variation between q and v which suggests the system is nearer to the voltage collapse point [30].

The participation factor of k^{th} bus in the i^{th} mode (P_{ki}) can be calculated using [30]:

$$P_{ki} = \zeta_{ki}\eta_{ki} \tag{7}$$

where ζ_{ki} and η_{ki} are the k^{th} element of i^{th} right eigenvector and left eigenvector respectively. Equation (7) helps to identify the bus that has a large contribution (participation factor) to the critical voltage stability modes of the system.

To identify, the critical line related to voltage stability, the participation factor of the line to the critical mode can be calculated as [3].

$$P_{li} = \frac{\Delta Q_{loss}\ for\ branch\ l}{max\ \Delta Q_{loss}\ for\ all\ branches} \tag{8}$$

where P_{li} is the contribution of the l^{th} line in the i^{th} critical voltage stability mode.

The higher the participation value of a line to the critical mode suggests that a large increment in reactive power loss occurs for a small increment in active power flowing through it; The large flow of reactive power in a transmission line is a possible early sign of a voltage collapse [3].

III. METHODOLOGY AND SYSTEM DESCRIPTION

A. METHODOLOGY

The methodology for assessing the power system stability of the power system stability of Nepal comprises three primary stages; The first stage involves modeling the transmission system, generator selection, and the dynamic components. The second stage encompasses the application of appropriate stability analysis methods and the final stage entails result analysis.

Data for the transmission lines, loads, and generators were sourced from [2]. All generators are modeled using a sixth-order model with default parameter values available in DIgSILENT. All the governors are assumed to be of IEEEG3 standard [31] and the excitation systems are based on IEEET1S [32]. Loads are represented as a combination of 70% static and 30% dynamic components with the static load model following the ZIP model. The transmission lines are modeled using the nominal π method.

The impact of RESs, mainly PVG on power system stability of the Nepal grid has also been studied in this paper. PVG was selected for the study due to its high feasibility within the country's context [33]. Additionally, PVG is the only RES besides hydropower which has been currently integrated in the power grid of Nepal. The PVG is modeled as described in [34].

Once the network is accurately modeled and the necessary components are selected, time-domain simulations are conducted to assess the transient and frequency stability. Modal analysis is applied for SSS analysis, and modal voltage stability analysis is used for static voltage stability assessment. The final stage involves the analysis of stability indices derived from the second stage. Various frequency stability indices, including f_{nadir}, maximum frequency (f_{max}), $RoCoF$, and angle stability indices, are analyzed. Additionally, critical buses and lines (identified based on participation factors) relevant to voltage stability are analyzed. All electrical analyses in this study are performed using the DIgSILENT software. A visual representation of the proposed stability assessment methodology is illustrated in Figure 1.

The proposed methodology also utilizes the sensitivity analysis to identify the power system parameters that have significant impact on the stability of the power grid of Nepal. The sensitivity analysis is performed using one at a time method as outlined in [35]. The output parameters are the sensitivity stability indices and the input parameters are the generation and load demand at the buses for this study. A new indices related to the sensitivity of the frequency stability

have been proposed as: df_{nadir}/dP_i where df_{nadir} is the change in the system COI nadir with respect to the base case; dP_i represents the change in the load or generation connected at the i^{th} bus compared to the base case. A higher value of this index indicate that the corresponding parameters are highly responsible for an under-frequency event. An increment of 1% is considered in P_i for this study. Similarly, $dTSI/dP_i$ is proposed for the transient stability analysis where $dTSI$ is the change in TSI compared to the base case. The buses (load and generator connected to it) with less values of it are critical with respect to the transient stability. The SSS sensitivity is calculated using $d\zeta_c/dP_i$ where $d\zeta_c$ denotes the change in damping ratio of the most critical mode compared to the base case. Lastly, dV_i/dP_i representing the change in voltage of the i^{th} bus with respect to the base case under power change at that bus has been used for voltage stability sensitivity analysis. A larger value of this index suggests that the system is operating nearer to the voltage collapse region [3].

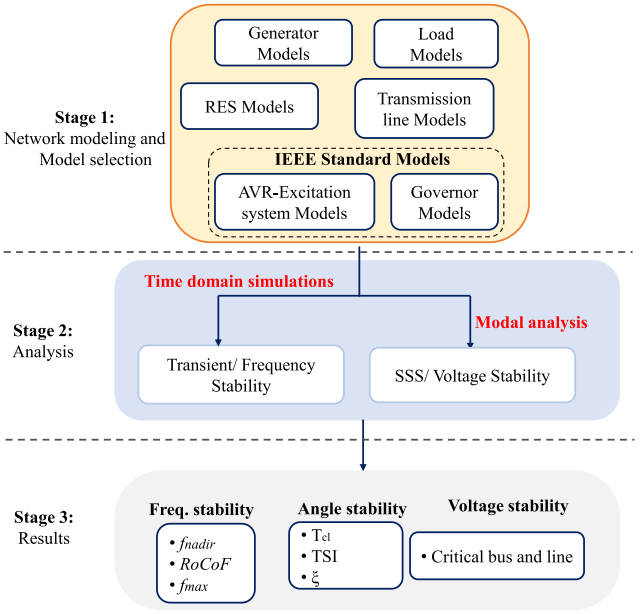

FIGURE 1. Proposed methodology for stability assessment of the power grid of Nepal.

B. SYSTEM DESCRIPTION

The power system of Nepal mainly consists of hydropower generations as shown in Figure 2. The modeled system comprises 101 buses, 34 generators and 53 loads. The total generation capacity and load for the modeled system are 1703.88 MW and 1544.31 MW, respectively. Voltage levels of 66 kV, 132 kV, 220 kV, and 400 kV (the highest voltage level in Nepal) have been considered. The model incorporates twenty-six 66 kV transmission lines with a total length of 521.56 km, sixty-two 132 kV transmission lines with a total length of 3019.9 km, four 220 kV transmission lines with a total length of 341.4 km, and one 400 kV transmission line with a total length of 60 km.

For simplicity, only generators with a capacity equal to or greater than 20 MW are considered in this study, aligning with the modeling approach employed by the NEA. Three connection points (Tanakpur, Balmikinagar, Muzaffarpur) link the power grid of Nepal to India. The Indian Grid (Muzaffarpur) is designated as the slack bus in this study. Detailed parameters for generators, lines, and loads, along with an overview of the modeled system are provided in the supplementary file (Tables S1-S4, Figures S1-S5).

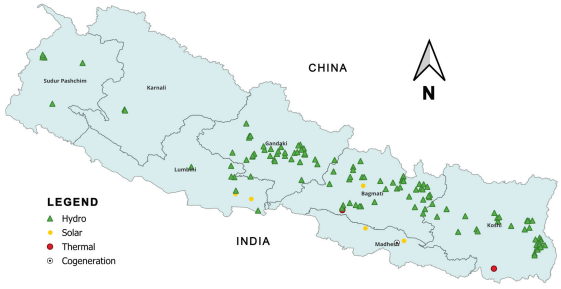

FIGURE 2. Major generating stations of Nepal.

IV. RESULTS AND DISCUSSION

This section presents the results obtained through the application of the proposed methodology described in Section III. Various stability indices related to angle, voltage, and frequency stability have been calculated. The results are analyzed under different scenarios as outlined in Table 1.

For Scenarios 2 and 3 (Table 1), load variations have been restricted to ±5% due to non-convergence of power flow beyond this range. Additionally, for the N-1 contingency condition (Loss of the highest loaded transmission line), the study considers the third highest loaded line, specifically the line connecting Patale and Kamane, as the power flow did not converge for the first two largest line outage conditions.

TABLE 1. Description of the scenarios considered in this paper.

Scenario	Name	Description
1	Base case	
2	Increased load condition	Load is increased by 5% to the base case
3	Decreased load condition	Load is decreased by 5% to the base case
4	N-1 contingency condition	Disconnection of line connecting Patale and Kamane

A. ANGLE STABILITY ANALYSIS RESULTS

1) SSS RESULTS

Table 2 displays the results obtained after performing eigenvalue analysis for the studied grid. The system exhibits two critical modes: one of local nature and the other inter-area. The local mode is influenced by the generators of Mistri Khola and Kaligandaki-A, while the inter-area mode involves generators from Nepal and India (specifically from

TABLE 2. SSS results under different scenarios.

Scenario	Mode No.	α (1/s)	Freq. (Hz)	$\zeta(\%)$	Participating states	Type
1	1	-0.2013	1.1256	2.846	Mistri Khola, Kaligandaki-A	Local
2	1	-0.1991	1.1174	2.8358		
3	1	-0.2029	1.1316	2.8535		
4	1	-0.2018	1.1235	2.8583		
1	2	-0.2065	0.7715	4.2570	India(Tanakpur), Marsyangdi-A, Mistri Khola, Mid Marsyangdi,Marsyangdi, Kaligandaki-A, India (Balmikinagar), Chilime	Interarea
2	2	-0.2375	0.7646	4.9391		
3	2	-0.1522	0.7788	3.1097		
4	2	-0.2231	0.7341	4.8314		

Balmikinagar and Tanakpur). Scenario 2 records the lowest damping ratio. Figure 3 shows the pictorial representation of the oscillatory instability vulnerable regions for the Nepal power grid.

FIGURE 3. Vulnerable areas concerning SSS.

2) TRANSIENT STABILITY RESULTS

The transient stability is assessed by introducing a self-clearing fault at the system's most critical line that is line connecting Khimti-Hydropower and Lamosangu station at 1 second. Table 3 presents the system's T_{cl} and TSI for all scenarios. The results reveal that the system loses transient stability at 0.55 seconds in the base case. Scenarios 2 and 4 exhibit the lowest T_{cl} and TSI values respectively, indicating a reduced transient stability margin under those conditions.

Figure 4 provides insights into generator rotor angles under the unstable conditions. The plot includes seven generators representing the largest generators in different regions of the power grid of Nepal. The generators of a particular region behave coherently and therefore only the largest generator of that region has been shown in the plots. Further details, including overshoot, undershoot, peak values, and settling times, are presented in Table 4. The results highlight that the generator at Modi experiences the highest overshoot and undershoot, while the generator at Chameliya records the longest settling time in response to a self-clearing fault at the critical line. Additional time response comparisons for other scenarios and plot under stable condition are provided in the supplementary file (Tables S5-S7, Figure S6).

The system T_{cl} and TSI are minimum under the increased load condition and N-1 contingency condition respectively, and may further degrade under the increased generation/load in the future. Hence, necessary measures such as fast circuit breakers, Flexible AC Transmission Systems (FACTS), and other transient stability enhancement devices must be installed to improve the transient stability margin of the Nepal's power system.

TABLE 3. Transient stability indices for different scenarios.

Scenario	$T_{cl}\,(s)$	$TSI\,(\%)$
1	0.55	82.6325
2	0.51	79.8336
3	0.52	85.7360
4	0.51	79.5869

TABLE 4. Time response comparison under base case.

No.	Generator	OS (%)	US (%)	Peak (deg.)	T_s (s)
1	Mai Khola	169.6846	10.8516	10.1295	16.2779
2	U Tamakoshi	19.6021	0	78.0034	10.3916
3	Kali Gandaki A	243.109	14.3023	35.1813	21.48
4	Chameliya	119.9672	0	50.3738	22.6868
5	Modi	250.7662	379.0415	16.8505	21.389
6	Mid Marsyanghdi	94.3038	97.4417	22.6025	20.1583

B. FREQUENCY STABILITY ANALYSIS RESULTS

The under-frequency event is studied by removing the largest generator, Upper Tamakoshi, at 1 second. Similarly, the removal of the largest load, Duhabi, is assumed at 1 second to study the over-frequency events. Both generator and load outages were applied separately for the analysis. Figure 5 illustrates the system's COI frequency under these outages for Scenarios 1-4. The plots indicate that the system's frequency remains well within the maximum allowed $\pm$ 2.5% criterion of the power system operator of Nepal, highlighting a substantial stability margin concerning frequency stability. The results provided by Table 5 demonstrate that the system's minimum and maximum frequency values are 49.3792 Hz to 50.1617 Hz respectively. Moreover, the extreme values of $RoCoF+$ (under generator outage) and $RoCoF-$ (under load outage) are 0.0477 Hz/s and 0.2083 Hz/s, respectively. These values conform to the allowable range of $\pm$0.5 Hz/s [27].

C. VOLTAGE STABILITY ANALYSIS RESULTS

As detailed in Section III, a static voltage stability analysis has been conducted to pinpoint the critical buses and lines within the power grid of Nepal concerning voltage stability. The results following the application of modal voltage

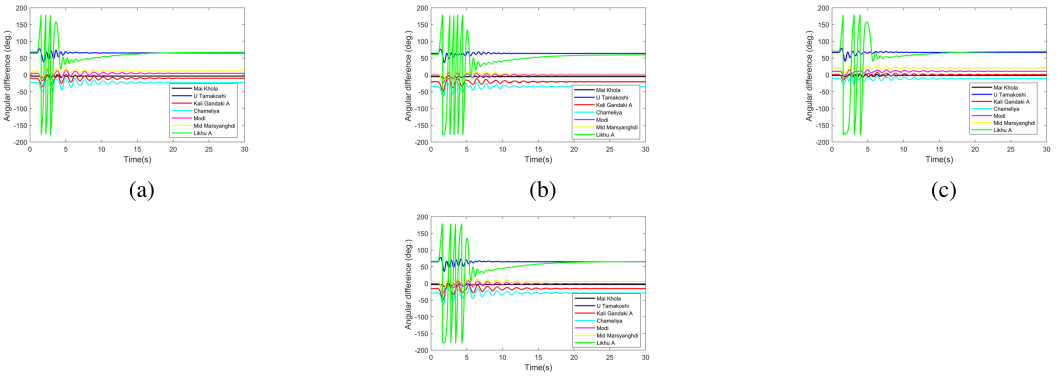

FIGURE 4. Time response of relative rotor angle of generators for (a) Scenario 1 (b) Scenario 2 (c) Scenario 3, and (d) Scenario 4 under transient unstable condition.

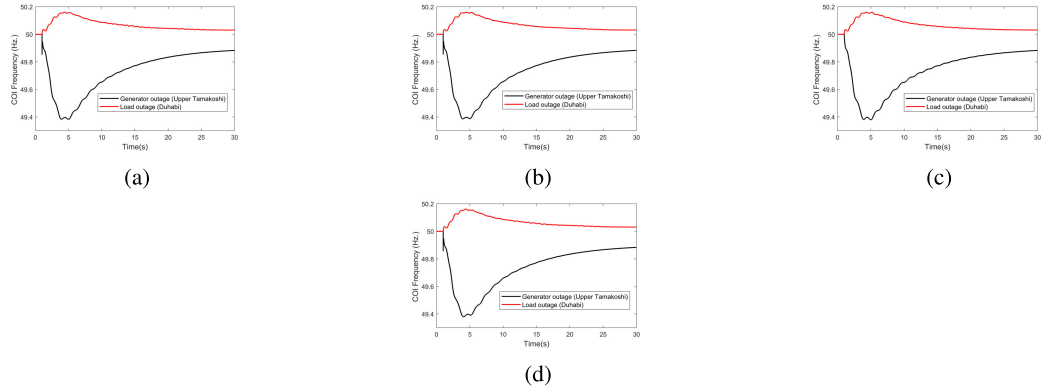

FIGURE 5. System COI frequency under outages for (a) Scenario 1 (b) Scenario 2 (c) Scenario 3, and (d) Scenario 4.

TABLE 5. Frequency stability indices for different scenarios.

Scenario	f_{nadir} $(Hz.)$	$RoCoF-$ (Hz/s)	f_{max} (Hz)	$RoCoF+$ (Hz/s)
1	49.3829	0.1543	50.1601	0.0472
2	49.3856	0.2083	50.1600	0.0377
3	49.3792	0.1551	50.1609	0.0381
4	49.3795	0.2021	50.1617	0.0477

TABLE 6. Five smallest eigenvalues for Scenario 1.

Mode no.	λ
1	24.59419577
2	89.20606601
3	182.4817518
4	353.3568905
5	357.1428571

stability analysis in the modeled system are presented in Table 6. This study focuses on the examination of the five critical modes for further analysis [3]. Especially, all identified modes exhibit positive characteristics and are notably distant from the origin, signifying a substantial voltage stability margin.

TABLE 7. Buses with the highest participation for smallest eigenvalues for Scenario 1.

Mode no.	Bus	Participation factor
1	Mai-Cascade-Khola-132 kV	0.1162
	Godak-132 kV	0.1153
	Phidim-132 kV	0.1152
	Mai-Khola-132 kV	0.1147
	Puwa-HEP-33 kV	0.1145
2	Sunkoshi-66 kV	0.3314
	Indrawati-66 kV	0.3177
	Paanchkhal-66 kV	0.2043
	Banepa-66 kV	0.1229
	Bhaktapur-66 kV	0.0235
3	Hapure-132 kV	0.1957
	Kusum-132 kV	0.1616
	Kohalpur-132 kV	0.1596
	Ghorahi-132 kV	0.1494
	Lamahi-132 kV	0.1414
4	Sunkoshi-66 kV	0.5061
	Indrawati-66 kV	0.4932
	Banepa-66 kV	0.0002
	Paanchkhal-66 kV	0.0002
	Bhaktapur-66 kV	0.0001
5	Balmikinagar-132 kV	0.3207
	Gandak-132 kV	0.2835
	Hongsi-Cement-132 kV	0.2147
	Bardghat-132 kV	0.1809

Subsequently, participation factor analysis has been executed for modes 1-5, yielding the outcome for the critical

TABLE 8. SSS results under different RES penetration levels.

RES Penetration (%)	Mode No.	α (1/s)	Freq. (Hz)	$\zeta(\%)$	Participating states	Type
3	1	-0.2005	1.1276	2.829		
10	1	-0.1943	1.1267	2.743		Local
15	1	-0.1922	1.1299	2.706	Mistri Khola, Kaligandaki-A	Local
20	1	-0.1777	1.1320	2.498		
3	2	-0.1787	0.7733	3.674	India(Tanakpur),	
10	2	-0.1591	0.7759	3.262	Marsyangdi-A, Mistri Khola, Mid-Marsyangdi, Marsyangdi	Interarea
15	2	-0.1462	0.7761	2.99	Kaligandaki-A, India (Balmikinagar), Chilime	
20	2	-0.0431	0.7807	0.0878		

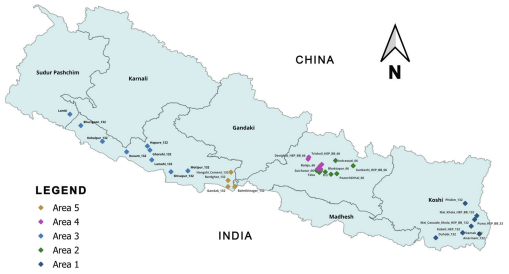

FIGURE 6. Vulnerable areas considering voltage stability.

bus as shown in Table 7. The results of the table reveals that the Mai-Cascade area exhibits the most substantial contribution to mode 1. In parallel, the Sunkoshi hydropower plant and its adjacent region significantly contribute to modes 2 and 4, while the Hapure area and its nearby vicinity make a significant contribution to mode 3. Table S8 in the supplementary file contains detail about the lines which have high participation to the critical modal voltage stability modes. The visual representation of regions vulnerable to voltage instability is shown in Figure 6. Similar results have been observed in scenarios 2 and 3 and are not presented in this section. However, the interested authors can find it in the supplementary file (Tables S9-S17).

D. RESULTS UNDER RES PENETRATION

The current PVG penetration (considering grid connected and of equal to or greater than 10MW) is only around 3% in the power grid of Nepal. This case is used as the initial base case for this section of the study. Furthermore, PVGs of varying sizes are added randomly in the southern belt of Nepal, primarily in the Madhesh province (Figure 2) as these regions are considered more feasible for harvesting PVG than other provinces [33]. Penetration rates of 3%, 10%, 15%, and 20% have been chosen for this study. Higher penetration rate beyond 20% has not been chosen as the current policy of GoN prioritizes the development of hydropower projects over other RESs as evident by the low PVG penetration in the current power grid of Nepal.

Table 8 shows the result of SSS analysis under different penetration level of RESs. The table shows that the damping ratio of both the critical modes deteriorates with the RES

TABLE 9. Transient stability indices under different RES penetration levels.

Scenario	$T_{cl}(s)$	$TSI\,(\%)$
3%	0.52	84.1578
10%	0.52	85.1225
15%	0.52	86.8164
20%	0.55	81.9450

TABLE 10. Time response comparison under 3% RES penetration.

No.	Generator	OS (%)	US (%)	Peak (deg.)	T_s (s)
1	Mai Khola	101.1241	0	11.1852	14.2091
2	U Tamakoshi	18.6968	0	78.4128	8.8253
3	Kali Gandaki A	350.0686	20.6969	26.3188	20.6246
4	Chameliya	124.2025	0	39.6087	21.1144
5	Modi	105.8346	137.3248	14.4221	19.8493
6	Mid Marsyanghdi	52.7426	26.5231	23.1868	19.2675

TABLE 11. Frequency stability indices under different RES penetration level.

RES (%)	f_{nadir} $(Hz.)$	$RoCoF-$ (Hz/s)	f_{max} (Hz)	$RoCoF+$ (Hz/s)
3	49.3813	0.1547	50.1663	0.0400
10	49.3809	0.1548	50.3371	0.0281
15	49.3811	0.1543	50.5830	0.0436
20	49.39	0.1506	50.8498	0.058

penetration level. Time domain simulations were conducted to obtain the critical clearing time and TSI values for different penetration level whose results are given in Table 9. The time response indices for the transient stable condition under 3% penetration level is shown in Table 9. The result shows that the overshoot and settling time all increases with the increase in RES penetration level. (See Tables S18-S20 in supplementary file for more time response indices and Figures S7-S8 for angular difference plots). An outage of the largest generator and largest load as in the previous section IV-B is done to observe the system COI frequency patterns. The resulting numerical outcome is summarized in Table 11. The value of f_{max} is maximum under 20% penetration level and the frequency nadir is minimum under 10% penetration level. The system RoCoF - seems to increase under 10% RES penetration level. The plots of COI frequency under different penetration level are provided in Figure S9 in the supplementary file. Lastly, the modal

voltage stability analysis was conducted to assess the voltage stability, with results presented in Table 12. All the modes demonstrate significant increase in their values with higher RES penetration level, signifying greater voltage stability margins. The results for the bus and branch participation are similar to the obtained in the section above and are omitted here for compactness.

TABLE 12. Five smallest eigenvalues concerning voltage stability under different RES penetration level.

Mode No.	λ			
	RES (3%)	RES (10%)	RES (15%)	RES (20%)
1	64.64121	64.5577	172.1170	185.1851
2	93.4579	93.63295	194.1747	194.1747
3	176.9911	173.9130	338.9830	338.9830
4	354.6099	355.8718	354.6099	636.9426
5	357.1428	357.1428	632.9113	704.2253

E. SENSITIVITY ANALYSIS RESULTS

The sensitivity analysis indices as described in Section III were calculated for the identification of critical areas with respect to the stability of the Nepal power grid. Table 13 represents the top five parameters which have the highest impact on stability of the power grid of Nepal.

The results in Table 13 indicate that generators such as lower Modi and those within that corridor are most critical with respect to the low-frequency oscillatory stability as they have the lowest value of $d\zeta_c/dP$. This finding aligns with the SSS results from Section IV-A1.

TABLE 13. Top five most important parameters impacting the Nepal power grid identified by the sensitivity analysis method.

Rank	$d\zeta_c/dP$	$dTSI/dP$	df_{nadir}/dP	dV/dP
1	Lower Modi	Modi	Amlekhjung	Indrawati
2	Modi	Syaule	Phidim	Sunkoshi
3	Upper Marsyangdhi	Chameliya	Bhurigaun	Panchkhal
4	Mid Marsyangdhi	Pahalmanpur	Mai Cascade	Anarmani
5	Tanakpur (India)	Lamki	Panchkhal	Puwa HEP

The transient stability sensitivity indices show that the Modi hydropower and electrical load at Syaule are the two most important contributors (lower $dTSI/dP$) in reduction of the transient stability margin. The sensitivity analysis related to voltage stability shows that the buses at Indrawati region and Puwa khola region (higher dV/dP) have a low voltage stability margin. This result is consistent to the voltage stability result of Section IV-C. Lastly, the sensitivity analysis conducted for the frequency stability shows that the load at Amlekjung (highest df_{nadir}/dP) has the most impact on under-frequency event.

V. DISCUSSION AND CONCLUSION

This paper analyzes the power system stability of the power grid of Nepal under different scenarios. The following points are the main findings of this work:

- The f_{nadir} and f_{max} for the power system of Nepal are 49.3792Hz and 50.1617Hz (Under the largest generator and load outage) respectively which are within the prescribed limits ($\pm$ 2.5%) by the Nepal Electric Authority. Similarly, the extreme values of $RoCoF+$ (under generator outage) and $RoCoF-$ (under load outage) are 0.0477Hz/s and 0.02083Hz/s respectively which lies within the allowed range of $\pm$ 0.5Hz/s. These results show that the Nepal power system is robust to the frequency instability issues. It can be expected due to the dominance of synchronous generator based generations and an extremely low share of variable RESs in the power grid of Nepal.
- The system's critical clearing time under fault at a critical line is approximately 0.51s.
- SSS analysis reveals the presence of two critical modes within the power system of Nepal, one with local characteristics and the other of inter-area nature. The study shows that the SSS margin is the most important stability for Nepal power grid in comparison to the other stability indices. The local mode exhibits the lowest damping ratio at approximately 2.8%. This value is low compared to the margins of most countries (typically 3-5% [36]). This problem worsens when RESs are added into the system. Thus, there is a high need to add PSSs at generators contributing to the critical modes such as Mistri Khola, Kaligandaki-A, Marsyangdhi etc.
- The voltage stability analysis results reveal that the Nepal grid has five potential voltage instability regions (Damak area, Bhaktapur area, Chahabil area, Hapure area, and Balmikinagar area).
- The scenarios marked by increased load conditions and N-1 contingency scenarios exhibit reduced stability margins for the Nepal power grid when compared to the base case and the decreased load condition.
- The addition of PVG decreases the SSS margin of both the critical modes and is lowest when the PVG penetration is 20%. Furthermore, the inter-area mode involving generator of neighbouring country i.e India becomes more dominant than the local mode under this penetration rate.
- The system voltage stability margin seems to improve with the addition of PVG in the Nepal power system. The RESs are mainly added at the southern belt of Nepal due to their higher feasibility there. As this province lacks any hydropower generating stations there, introduction of RES in this area shortens the distance between the source and the load center leading to a higher voltage stability margin under this scenario.
- The system transient stability margin as provided by the values of T_{cl} and TSI seems to be relatively similar to the other studied cases (Scenarios 1-4) under different penetration of RESs in the power grid of Nepal. However, the time domain simulations suggest that the power system variables (relative rotor angle, transmitted power, bus voltage) seem to show more

overshoot, undershoot and larger settling time under RES integration. This maybe due to the increase in power flow in transmission lines leading to the operation of the line at a higher power-angle under increased RES penetration level; This situation can cause the slow damping of power system oscillations resulting in larger overshoot and settling time.

- Fast-acting circuit breakers, FACTS devices and other transient stability enhancement devices need to be installed to improve the transient stability margin of the Nepal's power system.
- Reactive power compensating devices are suggested to be installed at the five potential voltage collapse areas to improve the voltage stability margin of the power grid of Nepal.
- The sensitivity analysis results show that the Modi hydropower and the electrical load at Syaule are the most critical with respect to the transient stability. Similarly, the result of the frequency stability sensitivity shows that the load connected at Amlekhjung contributes to the highest value and thus will be a suitable candidate for disconnection (if required) to prevent a severe under-frequency event.

This study, despite its best efforts, utilizes standard models of governor and excitation systems as most generating stations in Nepal do not log the actual parameter values for these controllers. Additionally, generators below 20 MW have not been considered for this study to reduce the complexity of the model of power grid of Nepal. The Nepal power system is continuously undergoing upgrades, which means this study cannot encompass all variables present in the actual power grid of Nepal. However, this paper serves as a comprehensive starting point for future research expansion in the power system stability domain of Nepal power grid. Our future studies will focus on developing solutions to address the stability issues identified in the Nepal power grid by this paper.

REFERENCES

[1] N. Hatziargyriou, J. Milanovic, C. Rahmann, V. Ajjarapu, C. Canizares, I. Erlich, D. Hill, I. Hiskens, I. Kamwa, B. Pal, P. Pourbeik, J. Sanchez-Gasca, A. Stankovic, T. Van Cutsem, V. Vittal, and C. Vournas, "Definition and classification of power system stability—Revisited & extended," *IEEE Trans. Power Syst.*, vol. 36, no. 4, pp. 3271–3281, Jul. 2021.

[2] *A Year in Review-Fiscal Year-2022/23*, NEA, Washington, DC, USA, 2023.

[3] P. S. Kundur, N. J. Balu, and M. G. Lauby, "Power system dynamics and stability," in *Power System Stability and Control*, vol. 3, 2017.

[4] T. Van Cutsem and C. Vournas, *Voltage Stability of Electric Power Systems*. Cham, Switzerland: Springer, 2007.

[5] S. Eftekharnejad, V. Vittal, G. T. Heydt, B. Keel, and J. Loehr, "Impact of increased penetration of photovoltaic generation on power systems," *IEEE Trans. Power Syst.*, vol. 28, no. 2, pp. 893–901, May 2013.

[6] S. Eftekharnejad, V. Vittal, G. T. Heydt, B. Keel, and J. Loehr, "Small signal stability assessment of power systems with increased penetration of photovoltaic generation: A case study," *IEEE Trans. Sustain. Energy*, vol. 4, no. 4, pp. 960–967, Oct. 2013.

[7] A. H. A. El-Kareem, M. A. Elhameed, and M. M. Elkholy, "Effective damping of local low frequency oscillations in power systems integrated with bulk PV generation," *Protection Control Modern Power Syst.*, vol. 6, no. 1, p. 41, Dec. 2021.

[8] W. Hu, Z. Lu, S. Wu, W. Zhang, Y. Dong, R. Yu, and B. Liu, "Real-time transient stability assessment in power system based on improved SVM," *J. Modern Power Syst. Clean Energy*, vol. 7, no. 1, pp. 26–37, Jan. 2019.

[9] Y. Lee and H. Song, "A reactive power compensation strategy for voltage stability challenges in the Korean power system with dynamic loads," *Sustainability*, vol. 11, no. 2, p. 326, Jan. 2019.

[10] Y.-B. Cho, Y.-S. Cho, J.-G. Lee, and S.-C. Oh, "Design and implementation of probabilistic transient stability approach to assess the high penetration of renewable energy in Korea," *Sustainability*, vol. 13, no. 8, p. 4205, Apr. 2021.

[11] O. Mogaka, R. Orenge, and J. Ndirangu, "Static voltage stability assessment of the Kenyan power network," *J. Electr. Comput. Eng.*, vol. 2021, pp. 1–16, Feb. 2021.

[12] B. B. Adetokun, J. O. Ojo, and C. M. Muriithi, "Application of large-scale grid-connected solar photovoltaic system for voltage stability improvement of weak national grids," *Sci. Rep.*, vol. 11, no. 1, Dec. 2021, Art. no. 24526.

[13] H. Jia, Q. Hou, P. Yong, Y. Liu, N. Zhang, D. Liu, and M. Hou, "Voltage stability constrained operation optimization: An ensemble sparse oblique regression tree method," *IEEE Trans. Power Syst.*, pp. 1–13, 2023.

[14] J. O'Sullivan, A. Rogers, D. Flynn, P. Smith, A. Mullane, and M. O'Malley, "Studying the maximum instantaneous non-synchronous generation in an island system—Frequency stability challenges in Ireland," *IEEE Trans. Power Syst.*, vol. 29, no. 6, pp. 2943–2951, Nov. 2014.

[15] G. Ben Yosef, A. Navon, O. Poliak, N. Etzion, N. Gal, J. Belikov, and Y. Levron, "Frequency stability of the Israeli power grid with high penetration of renewable sources and energy storage systems," *Energy Rep.*, vol. 7, pp. 6148–6161, Nov. 2021.

[16] J. Daković, M. Krpan, P. Ilak, T. Baškarad, and I. Kuzle, "Impact of wind capacity share, allocation of inertia and grid configuration on transient RoCoF: The case of the croatian power system," *Int. J. Electr. Power Energy Syst.*, vol. 121, Oct. 2020, Art. no. 106075.

[17] D. Guzs, A. Utans, A. Sauhats, G. Junghans, and J. Silinevics, "Resilience of the Baltic power system when operating in island mode," *IEEE Trans. Ind. Appl.*, vol. 58, no. 3, pp. 3175–3183, May 2022.

[18] H. Alsharif, M. Jalili, and K. N. Hasan, "Power system frequency stability using optimal sizing and placement of battery energy storage system under uncertainty," *J. Energy Storage*, vol. 50, Jun. 2022, Art. no. 104610.

[19] A. F. Heidari, A. Masoumzadeh, M. Vrakopoulou, and T. Alpcan, "Planning for inertia and resource adequacy in a renewable-rich power system," in *Proc. IEEE PES Innov. Smart Grid Technol. Asia (ISGT Asia)*, Nov. 2023, pp. 1–5.

[20] S. Ghimire, M. Ali, and D. Pozo, "Modal analysis for voltage-stable regime determination: The Nepalese power system case," in *Proc. Int. Youth Conf. Radio Electron., Electr. Power Eng. (REEPE)*, Mar. 2020, pp. 1–6.

[21] N. Regmi, S. K. Jha, S. Gurung, and D. Winkler, "Voltage stability assessment of eastern section of integrated Nepal power system," *Power*, vol. 2, p. E2, Jan. 2022.

[22] B. Pokhrel, "Analysis of small signal stability on wind power integration to integrated Nepal power system," Ph.D. dissertation, Pulchowk Campus, 2020.

[23] A. Parajuli, R. Shrestha, A. Adhikari, and S. Gurung, "Assessment of frequency and rotor angle stability of integrated Nepal power system," in *Proc. Int. Conf. Future Energy Solutions (FES)*, Jun. 2023, pp. 1–4.

[24] M. Basukala, N. Regmi, and S. Gurung, "Load frequency control of integrated Nepal power system," Tech. Rep., 2022.

[25] H. H. Alhelou, M. E. H. Golshan, T. C. Njenda, and N. D. Hatziargyriou, "An overview of UFLS in conventional, modern, and future smart power systems: Challenges and opportunities," *Electr. Power Syst. Res.*, vol. 179, Feb. 2020, Art. no. 106054.

[26] M. Sun, G. Liu, M. Popov, V. Terzija, and S. Azizi, "Underfrequency load shedding using locally estimated RoCoF of the center of inertia," *IEEE Trans. Power Syst.*, vol. 36, no. 5, pp. 4212–4222, Sep. 2021.

[27] M. O'Donovan, E. O'Callaghan, N. Barry, and J. Connell, "Implications for the rate of change of frequency on an isolated power system," in *Proc. 54th Int. Universities Power Eng. Conf. (UPEC)*, Sep. 2019, pp. 1–6.

[28] S. Gurung, F. Jurado, S. Naetiladdanon, and A. Sangswang, "Comparative analysis of probabilistic and deterministic approach to tune the power system stabilizers using the directional bat algorithm to improve system small-signal stability," *Electr. Power Syst. Res.*, vol. 181, Apr. 2020, Art. no. 106176.
[29] L. Shi, S. Dai, Y. Ni, L. Yao, and M. Bazargan, "Transient stability of power systems with high penetration of DFIG based wind farms," in *Proc. IEEE Power Energy Soc. Gen. Meeting*, Jul. 2009, pp. 1–6.
[30] G. K. Morison, B. Gao, and P. Kundur, "Voltage stability analysis using static and dynamic approaches," *IEEE Trans. Power Syst.*, vol. 8, no. 3, pp. 1159–1171, Jan. 1993.
[31] N. AG. (2015). *Turbine-Governor Models*. Accessed: Oct. 22, 2023. [Online]. Available: https://www.neplan.ch/wp-content/uploads/2015/08/Nep_TURBINES_GOV.pdf
[32] (2015). *Exciter Models*. Accessed: Oct. 22, 2023. [Online]. Available: https://www.neplan.ch/wp-content/uploads/2015/08/Nep_EXCITERS1.pdf
[33] D. Neupane, S. Kafle, K. R. Karki, D. H. Kim, and P. Pradhan, "Solar and wind energy potential assessment at provincial level in Nepal: Geospatial and economic analysis," *Renew. Energy*, vol. 181, pp. 278–291, Jan. 2022.
[34] B. Tamimi, C. Cañizares, and K. Bhattacharya, "System stability impact of large-scale and distributed solar photovoltaic generation: The case of Ontario, Canada," *IEEE Trans. Sustain. Energy*, vol. 4, no. 3, pp. 680–688, Jul. 2013.
[35] K. N. Hasan, R. Preece, and J. V. Milanovic, "Priority ranking of critical uncertainties affecting small-disturbance stability using sensitivity analysis techniques," *IEEE Trans. Power Syst.*, vol. 32, no. 4, pp. 2629–2639, Jul. 2017.
[36] P. Korba and K. Uhlen, "Wide-area monitoring of electromechanical oscillations in the Nordic power system: Practical experience," *IET Gener., Transmiss. Distrib.*, vol. 4, no. 10, p. 1116, 2010.

RASHNA SHRESTHA received the bachelor's degree in electrical engineering from the National College of Engineering, Tribhuvan University, in 2017, and the M.E. degree in electrical power engineering from Kathmandu University, Dhulikhel, Nepal, in 2023. She is currently with Nepal Electricity Authority. Her research interest includes power systems.

AMRIT PARAJULI received the bachelor's degree in electrical engineering from the National College of Engineering, Tribhuvan University, in 2019, and the M.E. degree in electrical power engineering from Kathmandu University, Dhulikhel, Nepal, in 2023. His research interests include the application of optimization methods and machine learning for enhancement of the power system stability.

MANISHA BASUKALA received the B.E. degree in electrical engineering from the Khwopa College of Engineering, Tribhuvan University, in 2017, and the M.E. degree in planning and operation of energy systems from Kathmandu University, in 2023. She is currently a Renewable Energy Engineer with Quasar Energy Consultants, Kathmandu, Nepal. Her research interests include the impact and mitigation of renewable energy resources on power systems.

SAMUNDRA GURUNG (Member, IEEE) received the B.E. degree in electrical and electronics engineering from Kathmandu University, in 2009, the M.E. degree in power systems engineering from the College of Engineering, Guindy, Anna University, in 2013, and the Ph.D. degree in electrical and computer engineering from the King Mongkut's University of Technology Thonburi, in 2019. He is currently an Assistant Professor with the Department of Electrical and Electronics Engineering, Kathmandu University. His research interests include power system stability and control, applied mathematics in power systems, and grid visualization.